Available online at www.sciencedirect.com
SCIENCE DIRECT®
Biochemical and Biophysical Research Communications 323 (2004) 453–464
BBRC
www.elsevier.com/locate/ybbrc

Transcriptional profiling of initial differentiation events in human embryonic stem cells

John D. Calhoun[a,1], Raj R. Rao[b,1], Susanne Warrenfeltz[d], Romdhane Rekaya[b,c], Stephen Dalton[b], John McDonald[d], Steven L. Stice[a,b,e,*]

[a] *Department of Biochemistry and Molecular Biology, The University of Georgia, Athens, GA 30602, USA*
[b] *Rhodes Animal Science Center, The University of Georgia, Athens, GA 30602, USA*
[c] *Department of Statistics, The University of Georgia, Athens, GA 30602, USA*
[d] *Department of Genetics, The University of Georgia, Athens, GA 30602, USA*
[e] *Georgia Tech/Emory Center for the Engineering of Living Tissues, 315 Ferst Drive, Atlanta, GA 30332, USA*

Received 26 July 2004

Abstract

Currently, there are no differentiation strategies for human embryonic stem cells (hESCs) that efficiently produce one specific cell type, possibly because of lack of understanding of the genes that control signaling events prior to overt differentiation. sed HepG2 cell conditioned medium (MEDII), which induces early differentiation in mouse ES cells while retaining pluripotent markers, to query gene expression in hESCs. Treatment of adherent hESCs with 50% MEDII medium effected differentiation to a cell type with gene expression similar to primitive streak stage cells of mouse embryos. MEDII treatment up-regulates *TDGF1* (Cripto), a gene essential for anterior–posterior axis and mesoderm formation in mouse embryos and a key component of the TGFB1/NODAL signaling pathway. LEFTYA, an antagonist of NODAL/TDGF1 signaling expressed in anterior visceral endoderm, is down-regulated with MEDII treatment, as is *FST*, an inhibitor of mesoderm induction via the related INHBE1 pathway. In summary, the TGFB1/NODAL pathway is important for primitive-streak and mesoderm formation and in using MEDII, we present a means for generating an in vitro cell population that maintains pluripotent gene expression (*POU5F1*, *NANOG*) and SSEA-4 markers while regulating genes in the TGFB1/NODAL pathway, which may lead to more uniform formation of mesoderm in vitro.
© 2004 Elsevier Inc. All rights reserved.

Keywords: Embryonic stem cell; Human; Hepatocellular carcinoma; Cripto; Pluripotency; Mesoderm

Significant research efforts have focused on developing hESC differentiation strategies [1], but successful in vitro differentiation will require a well-characterized starting pluripotent hESC population. Changes in hESC gene expression, without an alteration in overt pluripotent characteristics or markers in hESCs, may uncover or further define pathways and mechanisms involved in maintenance and then initial loss of pluripotency. We believe a detailed understanding of these mechanisms will be essential for developing hESCs as in vitro models for human embryonic development and for harnessing the differentiation capacity that makes hESCs an attractive starting material for cellular replacement therapy.

Many recent reports have used microarray technology to characterize the transcriptional profile of hESCs [2–5]. These studies indicate that like mES cells, there is a set of genes expressed in hESCs that are down-regulated upon differentiation [3–5] or expressed exclusively in hESCs in comparison to somatic, or non-pluripotent, cell types [6].

* Corresponding author. Fax: +1 706 542 7925.
E-mail address: sstice@uga.edu (S.L. Stice).
[1] The authors wish it to be known that, in their opinion, the first two authors should be regarded as joint first authors.

0006-291X/$ - see front matter © 2004 Elsevier Inc. All rights reserved.
doi:10.1016/j.bbrc.2004.08.117

During early mouse embryonic development, inner cell mass (ICM) cells, the in vivo equivalent of ES cells, undergo differentiation to a second pluripotent cell population termed primitive ectoderm. Primitive ectoderm is characterized by continued expression of pluripotency markers such as POU5F1 and alkaline phosphatase (AP) and increased expression of fibroblast growth factor 5 (FGF5) [7]. Upon exposure to a HepG2 cell conditioned medium, termed MEDII, mouse ES cells (mESCs) mimicked differentiation to primitive ectoderm in vitro [8]. Further studies demonstrated that MEDII could also enhance differentiation of adherent mESCs toward mesoderm [9] or aggregated mESCs to neurectoderm [10]. We have also demonstrated recently that the effect of MEDII can be translated to primate ES cells. MEDII enhanced the differentiation of aggregated monkey [11] and hESCs [12] towards neural fates. However, these experiments did not investigate MEDII's effect on early ES differentiation events, specifically in adherent cultures. In this study, our aim was to better characterize the pluripotent state of adherent hESCs and the effect of MEDII on early developmental differentiation events in hESCs.

In this current study, we compare hESCs cultured with and without MEDII, to ascertain early gene expression patterns associated with a treatment previously used to induce primitive ectoderm formation in mESCs. Using a combination of different experimental approaches, we have evaluated cellular morphology, cell cycle characteristics, immunostaining, and gene expression of adherent hESCs in response to MEDII. Human ES cells responded to MEDII treatment in a manner similar to mESCs. Both hESCs and MEDII-treated hESCs have a cell cycle profile similar to that of mESC and MEDII-treated mESCs. Like their murine counterparts, hESCs treated with MEDII expressed pluripotency markers yet exhibited differential gene expression in comparison to hESCs. There were key changes in genes expressed during early embryonic development in these two hESC cell populations. Specifically, teratocarcinoma-derived growth factor 1 (TDGF1, cripto), a co-receptor and agonist of INHBE1/NODAL/TGFB1 pathway, was up-regulated upon MEDII treatment, suggesting that MEDII may aid in the activation of this signaling pathway. Two antagonists of this signaling pathway, LEFTYA and *FST* (Follistatin), were downregulated upon MEDII treatment. *GATA6*, *TBX1*, and *ZNF1A1* (Ikaros), all markers of developing mesoderm in the mouse embryo, were also up-regulated in response to MEDII treatment. Taken together, all of these gene expression changes suggest that treatment with MEDII influences differentiation towards mesoderm in adherent hESC cell culture. This is the first study suggesting that MEDII conditioned medium affects components of the TGFB1/NODAL pathway in ES cells of any species.

Materials and methods

Human ES cell culture. BG01 human ES cells [13] were maintained on mitomycin C inactivated mouse embryonic feeder (MEF) layers in DMEM/F12, 20% Knockout Serum Replacer, 2 mM L-glutamine, 0.1 mM MEM non-essential amino acids, 50 U/ml penicillin, 50 μg/ml streptomycin (all from Gibco/Invitrogen), 1000 U/ml hLIF (Chemicon), 0.1 mM βME (Sigma), and 4 ng/ml bFGF (Sigma). Cells were passaged with 0.05% trypsin–EDTA (Invitrogen) every three days and re-plated on fresh feeder layers. For microarray analysis, parallel cultures were plated in either growth media (ES) or growth media supplemented with 50% MEDII medium (Fig. 3).

Generation of serum free MEDII conditioned medium. MEDII medium was prepared as described previously [8]. Briefly, HepG2 cells were maintained in DMEM/F-12 medium supplemented with 10% FBS, 1× L-glutamine, and 1× Pen-Strep. HepG2 cells were plated at a density of 16.5 times 10^6 cells in a 175 cm^2 flask. After three days of culture, serum containing growth medium was aspirated, cells were rinsed once with PBS and fed with 50 ml HepG2 growth media that lacked serum. After three days, media was collected, centrifuged to remove any non-adherent cells, and filter-sterilized. Serum free MEDII medium was stored at 4 °C until use.

Immunostaining of adherent hESC and MEDII-treated hESCs. Human ES cells and MEDII-treated hESCs were plated on 4-well Permanox Chamber slides (Nalgene) that had previously been seeded with mitomycin C inactivated MEF feeder layers. Cells were plated at 30,000 cells per chamber and grown in either hESC growth medium or hESC growth medium supplemented with 50% MEDII conditioned medium. After three days of culture, medium was aspirated, cells were rinsed once with PBS and fixed by incubation with 4% paraformaldehyde 4% sucrose solution for 15 min at room temperature, followed by several rinses with PBS.

For POU5F1 staining, cells were permeabilized and blocked by incubation in 1.5 T (50 mM Tris, pH 7.6, 250 mM NaCl) containing 3% normal goat serum, 0.3% Triton X-100, and 1% polyvinyl pyrolidine for 30 min. Cells were then incubated with primary antibody (Santa Cruz Biotechnology, 1:500 dilution) in blocking and permeabilization buffer for 1 h. After three washes in 1.5 T with 0.05% Tween 20 (Sigma), cells were incubated with an Alexa 488 conjugated secondary antibody (1:1000 dilutions, Molecular Probes) for 1 h in blocking and permeabilization buffer. Subsequently, cells were washed 3× in 1.5 T with 0.05% Tween 20 and nuclei were stained with DAPI (1 μg/ml, Roche).

For SSEA-4 staining, cells were incubated in blocking solution (PBS with 3% normal goat serum) for 45 min at room temperature. Cells were then incubated with primary antibody (Chemicon, 1:1000 dilution) in blocking solution for 30 min at room temperature. After three washes with PBS, cells were incubated with an Alexa 488 conjugated secondary antibody (Molecular Probes, 1:1000 dilution) in blocking solution for 30 min at room temperature. Subsequently, cells were washed 3× in 1.5 T with 0.05% Tween 20 and nuclei were stained with DAPI (1 μg/ml, Roche). Cells on slides were later visualized on a Nikon TE 2000-E inverted microscope using fluorescence microscopy.

Suspension staining and cell cycle analysis of adherent hESC and MEDII-treated hESCs. For suspension staining, hESCs were harvested from adherent culture with 0.05% trypsin–EDTA (Invitrogen), centrifuged at 1000 rpm at 4 °C, and re-suspended in suspension staining buffer consisting of PBS with 0.5 mM EDTA and 3% normal goat serum. After re-suspension in staining buffer, all the subsequent incubation steps involved cells being kept at 4 °C. Cells were then incubated in anti-SSEA-4 (Chemicon, 1:200 dilution) at 4 °C for 15 min. Cell suspensions were washed two times in staining buffer and collected by centrifugation before re-suspension in an Alexa 488 conjugated secondary antibody (Molecular Probes, 1:1000 dilution) in staining buffer. Cells were incubated for 15 min at 4 °C and washed twice with staining buffer. The cells were later fixed by re-suspension in

70% EtOH and stored at −20 °C until they were analyzed on a Becton–Dickinson FACSCalibur flow cytometer.

For cell cycle analysis, samples that had been suspension stained for SSEA4 and stored at −20 °C in 70% EtOH were washed several times to remove residual EtOH and re-suspended in a solution of 50 μg/ml RNase A and 50 μg/ml propidium iodide. Samples were then analyzed by flow cytometry and all data analysis was done using FloJo software.

Microarray analysis of hESC and MEDII-treated-hESCs. In preparation for microarray analysis, parallel cultures of untreated hESCs and hESCs treated with 50% MEDII were obtained as illustrated in Fig. 3A. The treatment was performed over three sequential independent passages and hybridized to six Affymetrix HG-U133A chips to ensure reproducibility of the response to MEDII. At each three day interval, cultures of untreated and treated cells were harvested, re-suspended in 1 ml Trizol (Invitrogen), and triturated until homogenized. Samples were stored at −80 °C until all six samples were prepared. RNA was isolated from the crude homogenate according to the manufacturer's protocols (Trizol, Molecular Research) using linear polyacrylamide (5 μl) to aid in RNA precipitation. Total RNA was further purified with RNAEasy (Qiagen) using the manufacturer's cleanup protocol. RNA quality was assessed by gel electrophoresis and only high quality RNA displaying no degradation by gel electrophoresis, a 2:1 ratio of ribosomal bands, and an A_{260}/A_{280} ratio of 1.9–2.1 was used for biotinylated target preparation.

Biotinylated target cRNA was generated according to the Affymetrix Technical Manual. Briefly, 10 μg total RNA was converted to double stranded cDNA using Superscript II (Invitrogen). The cDNA was cleaned by phenol/chloroform extraction and ethanol precipitation. In vitro transcription of the cDNA with the High Yield RNA Transcript Labeling Kit (Enzo) yielded 50–100 μg of biotin labeled cRNA target. The cRNA was fragmented in metal catalyzed acid hydrolysis to a length of 20–200 bp (by electrophoresis) and the fragmented cRNA was hybridized to the Affymetrix HG U133A array for 16 h at 45 °C. Hybridized arrays were washed, stained, and scanned according to the Affymetrix technical manual.

For data analysis, .DAT files were converted to .CEL files using Affymetrix MAS 5.0 software. Using the Affy package of Bioconductor (http://www.bioconductor.org), background correction was performed on. CEL files using the background correct function of the RMA algorithm [14]. Perfect match (PM) probe level data were then outputted as a text file. For this study, mismatch (MM) probe data were not used for differential gene expression analysis. PM probe data of the treated and untreated samples were then analyzed using a mixed linear model to determine differential gene expression [15]. It is important to note that once data have been processed in the model, differences in fluorescence intensity between treated and untreated array data should be due to the treatment alone.

The following mixed linear model was used to analyze the probe level intensities for every gene separately:

$$y_{ijkl} = T_i + P_j + TP_{ij} + t_l + t_l * P_j + T_i * P_j + t_l * T_i + A_k + e_{ijkl},$$

where y_{ijkl} is the transformed $\log_2$ expression intensity generated under treatment (T) i ($i = 1, 2$) at the jth ($j = 1, 2, \ldots, 20$) probe (P) in the array (A) k ($k = 1, 2, \ldots, 6$) at the passage time (t) l ($l = 1, 2, 3$). It is important to note that the number of probes per gene ranged from 11 to 20.

Furthermore, the following assumptions were made about the distribution of the random effects in the model:

$$e_{ijkl}|\sigma_e^2 \sim N(0, \sigma_e^2); \quad A_k|\sigma_a^2 \sim N(0, \sigma_a^2),$$

where σ_e^2 and σ_a^2 are the within and between array variances, respectively. Further, those two parameters were assumed unknown and were inferred from the data using maximum likelihood based methods.

Data for each of the 22,215 genes were processed on a gene-by-gene basis simultaneously. Since 22,215 tests were run simultaneously, a Bonferroni adjusted p value (i.e., 0.05/22,215) was considered to be the measure of stringency to minimize false positive results in the data set. Genes that met the Bonferroni criteria were the primary focus of the study; however this criterion was relaxed to a p value of 0.001 to increase the data set for a more generalized understanding of the differential expression patterns. Ontologies were processed using the NetAffx (http://www.affymetrix.com) software.

Real-time PCR confirmation of differentially expressed genes. Differentially expressed genes to be confirmed by real-time PCR were chosen by three criteria: a p value well within the Bonferroni cutoff, a high fold change, and the relevance of the gene to developmental processes. Accordingly, homeobox A1 (*HOXA1*), dapper (*DACT1*), Follistatin (*FST*), and Enhancer of Zeste homolog 2 (*EZH2*) were chosen as genes down-regulated with MEDII treatment (hESC cell enriched). *TDGF1* was chosen as an up-regulated gene (MEDII enriched). *POU5F1* and *NANOG*, markers of pluripotency that are not differentially expressed between the two populations, were assessed as treatment controls. Sequence information was obtained by interrogating probe information in the NetAffx online analysis software (Affymetrix) and following appropriate links to Ensembl (http://www.ensembl.org) web pages. Sequence information was loaded into Biology Workbench (http://workbench.sdsc.edu) and PRIMER 3 was used to design primers that spanned intron exon boundaries. RNA in excess from isolations for microarray analysis was reverse transcribed using the SuperScript III First-Strand Synthesis System (Invitrogen) according to manufacturer's protocol. Real-Time PCR was done on an Applied Biosystems' ABI PRISM 7700 Sequence Detection System using SYBR Green PCR Core Reagents according to manufacturer's protocols (http://www.appliedbiosystems.com). Data analysis was performed with the REST software package (http://www.gene-quantification.info/).

Results

MEDII treatment altered adherent hESC colony morphology

After treatment with MEDII, adherent hESCs were flatter than their non-treated counterparts and appeared to have less intercellular space (Figs. 1A and B). However, MEDII-treated hESCs continued to grow in colonies and their morphology was distinctly different from that of spontaneously differentiated cells seen routinely in the laboratory (Figs. 1C and D). We have also observed that MEDII-treated hESCs were more resistant to dissociation than untreated hESC cell colonies and may have formed tighter connections among cells within the colony.

MEDII treatment did not alter pluripotent marker expression or cell cycle profile in hESCs

To characterize the effect of MEDII on adherent hESCs, immunostaining with known hESC markers was carried out. BG01 hESCs exhibited stable and uniform stage-specific embryonic antigen 4 (SSEA-4) and POU5F1 protein expression during continuous culture (Figs. 1F, H, J, and L). At each stage of passaging during the experiment, parallel cultures of hESCs were plated for assessment of SSEA-4 expression levels. As seen in Fig. 2, both hESC cell and MEDII-treated hESCs

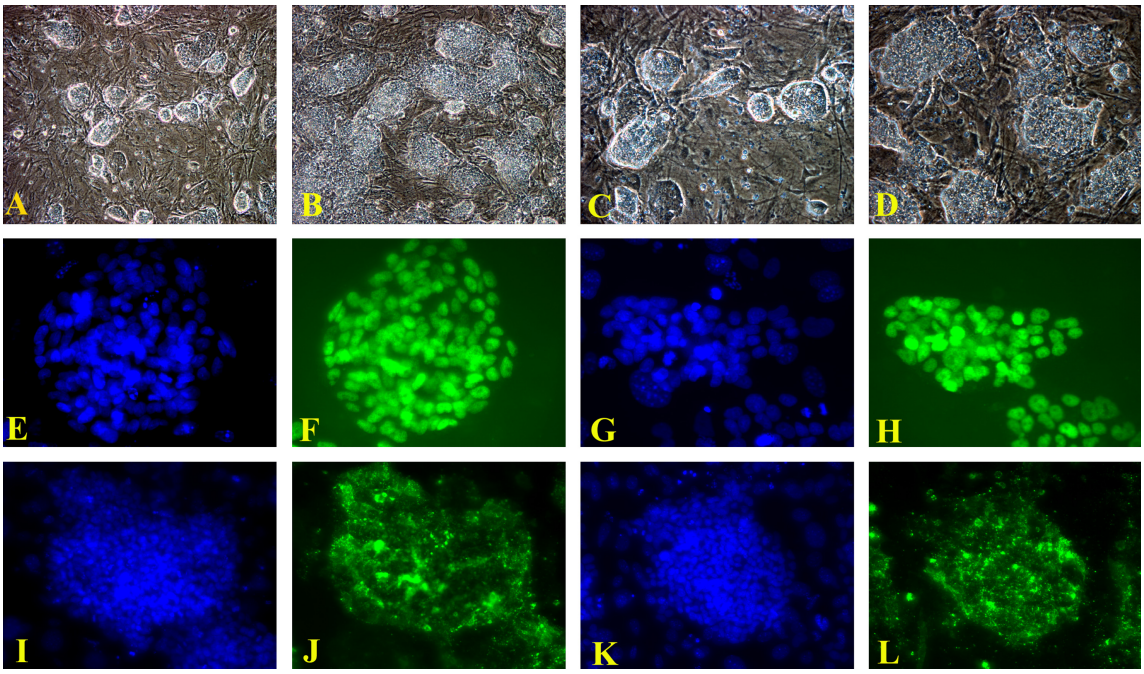

Fig. 1. MEDII treatment effects a morphological change in hESCs without loss of pluripotency. Phase contrast images of control (A,C) and MEDII (B,D) treated hESCs. (E) DAPI and (F) POU5F1 staining of control hESCs. (G) DAPI and (H) POU5F1 staining of MEDII-treated hESCs. (I) DAPI and (J) SSEA-4 staining of control hESCs. (K) DAPI and (L) SSEA-4 staining of MEDII-treated hESCs. Magnifications: (A,B) 100×, (C,D) 200×, and (E–L) 400×.

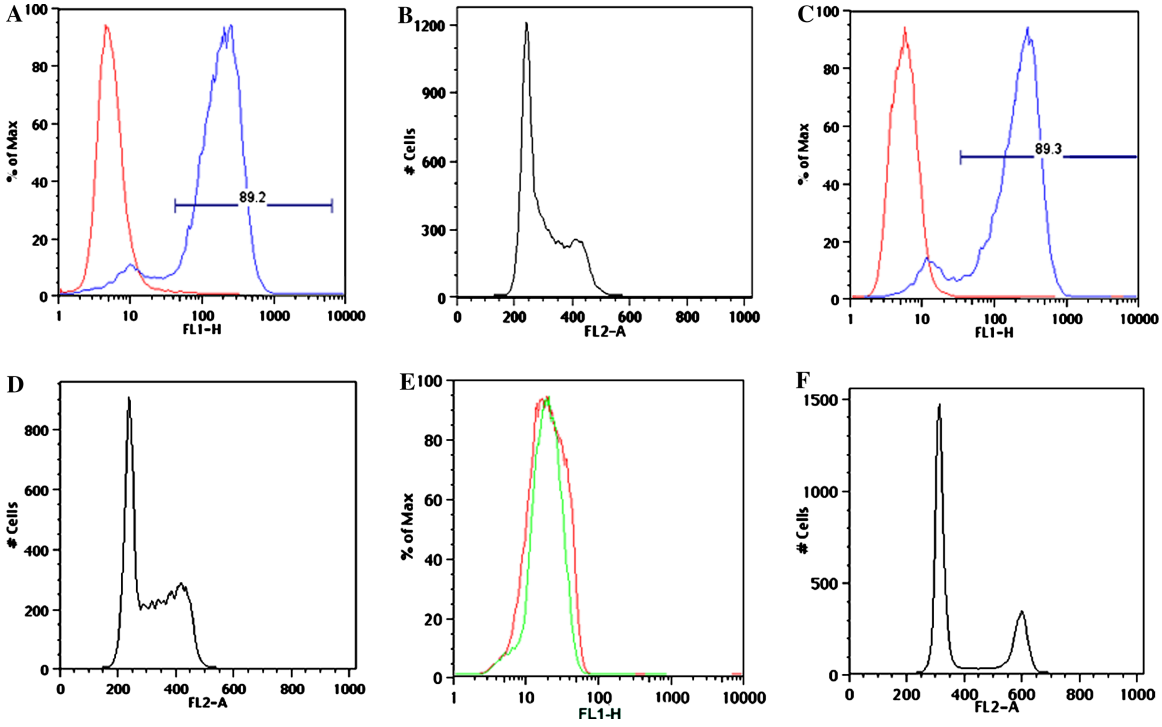

Fig. 2. Untreated and MEDII-treated hESCs have similar cell cycle profiles. Flow cytometry profile of untreated (A) and MEDII treated (C) hESCs stained for SSEA-4 expression. Red trace represents staining done with secondary antibody alone and blue trace represents staining done with both primary and secondary antibody. Cell cycle profiles of untreated (B) and MEDII treated (D) hESCs after gating to remove dead cells, doublets, and non-SSEA-4 positive cells. SSEA-4 staining (E) and cell cycle profile (F) of control mouse embryonic fibroblasts. Green trace represents staining done with secondary antibody alone and red trace represents staining done with both primary and secondary antibody. (For interpretation of the references to colour in this figure legend, the reader is referred to the web version of this paper.)

exhibited a large shift in fluorescence intensity (blue traces, Figs. 2A and C) over hESCs or MEDII treated hESCs incubated with secondary antibody only (red traces, Figs. 2A and C). A shift was not seen in the negative control of MEF cells since there was no difference between MEF cells incubated with secondary antibody alone (green trace, Fig. 2E) and MEF cells incubated with both primary and secondary antibody (red trace, Fig. 2F).

Cell cycle analysis was performed on adherent hESC cell and MEDII treated hESCs. The BG01 hESCs used in this study displayed a pluripotent cell cycle profile with a high percentage of cells occupying the S and G2/M phases of the cell cycle (Fig. 2B). MEDII treatment did not significantly change the cell cycle profile of treated cells (Fig. 2D). The treated cells continued to display a pluripotent cell cycle profile with many cells occupying the S and G2/M phases of the cell cycle. In contrast, significantly fewer control MEF cells occupy the S and G2/M phases of the cell cycle (Fig. 2F), with the population exhibiting a cell cycle structure consistent with that of proliferating somatic cells in culture.

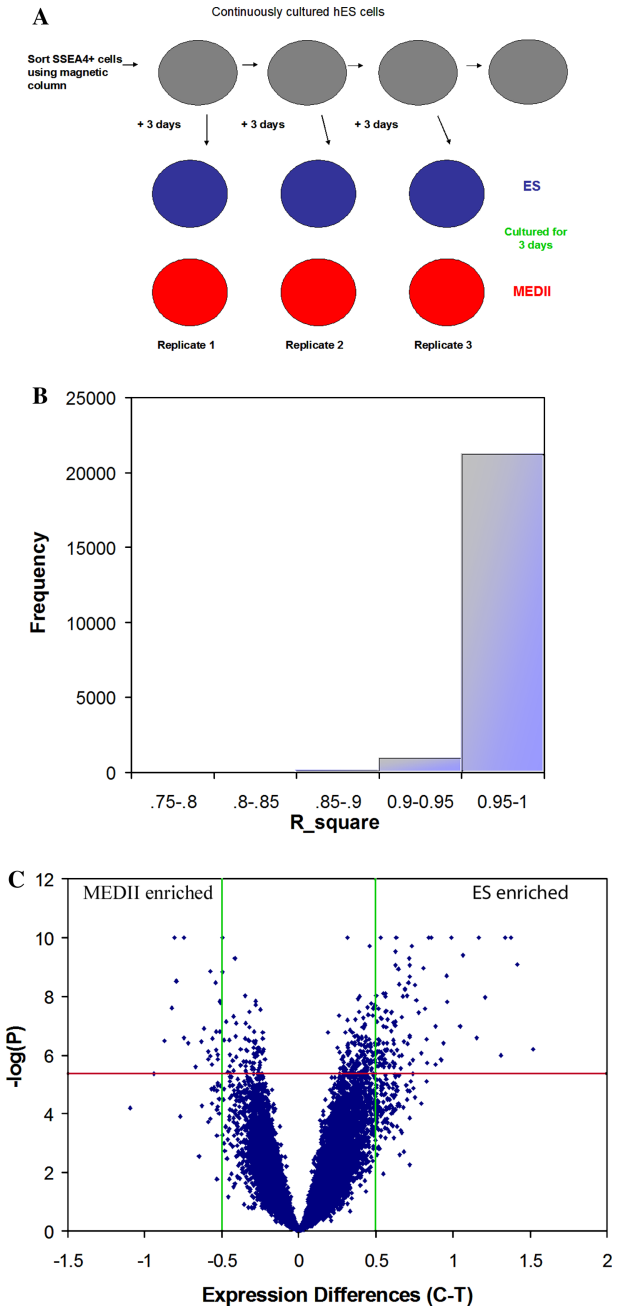

Fig. 3. Microarray analysis of untreated and MEDII-treated hESCs. (A) Schematic detailing the experimental strategy employed for the microarray experiments. (B) Histogram of R^2 values from mixed linear model for each of the 22,215 genes characterized. (C) Volcano plot of p value vs. difference in expression value for all 22,215 genes analyzed by microarray between control and treated hESCs. The x-axis is the $\log_2$ estimate of the difference of levels in the MEDII treatment. The y-axis is the negative log p value.

MEDII causes changes in gene expression but not in pluripotency genes

The global gene expression profiles of untreated and MEDII-treated adherent hESCs were compared by microarray analysis. It is important to note that the R^2 values, a determination of goodness-of fit for each of the genes, ranged between 0.95 and 0.99, indicating that the mixed linear model adopted fits the data from almost all genes very well (Fig. 3B). A plot of difference in gene expression between MEDII-treated and -untreated hESCs versus the negative log base 2 ($\log_2$) transformed p value (volcano plot) shows the behavior of all genes analyzed (Fig. 3C). A larger number of genes in the hESC enriched quadrant of the volcano plot suggest that more genes were downregulated in hESCs in response to MEDII than were up-regulated by MEDII treatment. This is also reflected in the statistical summary table (Table 1). Focusing on genes that meet the stringent Bonferroni criterion and a fold change greater than 1.5, 73 genes were down-regulated

Table 1
Summary of statistics for microarray analysis of gene expression

SigLevel[a]	Bonferroni	0.001	0.01	0.05
N(up)[b]	83	1044	2796	5012
FC(up)[c]	1.38	1.24	1.21	1.2
N(Dn)[b]	203	1499	2804	4355
FC(Dn)[c]	1.62	1.37	1.31	1.28
Fc(All)[c]	1.55	1.32	1.26	1.24
%Up[d]	29	41	50	54
%Dn[e]	71	59	50	46
%Genes[f]	1.3	11.4	25.1	42.1

[a] Significance level.
[b] No. of genes up or downregulated at indicated significance level.
[c] Fold changes up or down.
[d] Percent of genes that are upregulated.
[e] Percent of genes that are downregulated.
[f] Percent of all genes on the microarrays that are differentially expressed.

Table 2
Genes down-regulated after MEDII treatment of hESC

Functional category	Gene symbol	Gene description	Locus	Fold change
Calcium binding	VSNL1	Visinin-like 1	2p24.3	1.98
Cell adhesion	CNTNAP2	Contactin-associated protein-like 2	7q35–q36	2.27
	JUP	Junction plakoglobin	17q21	1.96
Cell cycle	MAD2L1	MAD2 mitotic arrest deficient-like 1	4q27	1.75
Cell growth/maintenance	C6.1A	C6.1A	Xq28	2.13
	PRCC	Papillary renal cell carcinoma (translocation-associated)	1q21.1	1.80
	MTM1	Myotubular myopathy 1	Xq28	1.60
	ARK5	AMP-activated protein kinase family member 5	12q24.11	1.60
	AF1Q	ALL1-fused gene from chromosome 1q	1q21	1.55
Cell proliferation	PTCH	Patched	9q22.3	2.50
	TGFB1	Transforming growth factor, β1	19q13.2	2.15
	GPC4	Glypican-4	Xq26.1	2.13
Chromosome organization	H2BFB	Histone 1, H2bd	6p21.3	2.11
	EZH2	Enhancer of zeste homolog 2	7q35–q36	1.94
Cytoskeletal-related	NEF3	Neurofilament 3	8p21	7.50
	NEFL	Neurofilament, light polypeptide 68 kDa	8p21	5.13
	KIAA1102	KIAA1102 protein	4p14	2.30
	TPM2	Tropomyosin 2	9p13.2–p13.1	1.52
Development	FST	Follistatin	5q11.2	2.59
DNA binding	LHFP	Lipoma HMGIC fusion partner	13q12	2.73
	CSTF2T	Cleavage stimulation factor, subunit 2	10q11	2.32
	BTF	BCL2-associated transcription factor 1	6q22–q23	2.08
	NBS1	Nijmegen breakage syndrome 1 (nibrin)	8q21	2.05
	PDCD2	Programmed cell death 2	6q27	1.95
DNA repair	MBD4	Methyl-CpG-binding domain protein 4	3q21–q22	1.75
DNA replication	ORC5L	Origin recognition complex, subunit 5-like	7q22.1	1.54
Electron transport	GLRX2	Glutaredoxin 2	1q31.2–q31.3	2.22
Heat shock protein activity	HSPA6	Heat shock 70 kDa protein 6	1q23	1.59
Metabolism	CA2	Carbonic anhydrase II	8q22	3.17
	ME1	Malic enzyme 1	6q12	3.16
	GAD1	Glutamate decarboxylase 1	2q31	2.04
	ASS	Argininosuccinate synthetase	9q34.1	2.01
	LEPREL1	Leprecan-like 1	3q29	1.66
	SLC7A5	Solute carrier family 7, member 5	16q24.3	1.62
	GAD1	Glutamate decarboxylase 1	2q31	1.61
	ODC1	Ornithine decarboxylase 1	2p25	1.59
Metal ion binding	MT2A	Metallothionein 2A	16q13	1.71
	MT1L	Metallothionein 1L	16q13	1.58
Protein biosynthesis	RPL27	Ribosomal protein L27	17q21.1–q21.2	1.80
Protein folding	DNAJC7	DnaJ (Hsp40) homolog, subfamily C, member 7	17q11.2	1.84
Respiratory gaseous exchange	HNMT	Histamine *N*-methyltransferase	2q22.1	1.75
RNA splicing	DDX23	DEAD (Asp-Glu-Ala-Asp) box polypeptide 23	12q13.12	2.56
	SFRS2	Splicing factor, arginine/serine-rich 2	17q25.3	1.68

Table 2 (*continued*)

Functional category	Gene symbol	Gene description	Locus	Fold change
Signaling	FLJ23091	Putative NFκB activating protein 373	1p31.2	4.97
	DACT1	Dapper homolog 1	14q23.1	2.38
	EFNA4	Ephrin-A4	1q21–q22	1.90
	WNT5A	Wingless-type MMTV integration site family, member 5A	3p21–p14	1.81
	EBAF	Endometrial bleeding associated factor	1q42.1	1.79
	MPP6	Membrane protein, palmitoylated 6	7p15	1.66
	CXCL14	Chemokine (C-X-C motif) ligand 14	5q31	1.65
	ARL7	ADP-ribosylation factor-like 7	2q37.2	1.53
Transcriptional regulation	HOXA1	Homeo box A1	7p15.3	4.61
	LEF1	Lymphoid enhancer-binding factor 1	4q23–q25	2.76
	ZNF84	Zinc finger protein 84	12q24.33	2.49
	ARNTL	Aryl hydrocarbon receptor nuclear translocator-like	11p15	2.37
	TFB2M	Transcription factor B2, mitochondrial	1q44	1.82
	CITED2	Cbp/p300-interacting transactivator, 2	6q23.3	1.63
	PWP1	Nuclear phosphoprotein similar to *S. cerevisiae* PWP1	12q24.11	1.50
Translation	EIF5	Eukaryotic translation initiation factor 5	14q32.33	2.56
Tumor antigen	PNMA1	Paraneoplastic antigen MA1	14q24.2	1.88
Unknown	BAG5	BCL2-associated athanogene 5	14q32.33	3.09
	FLJ12750	Hypothetical protein FLJ12750	12q24.31	2.68
	FLJ20516	Timeless-interacting protein	15q22.2	1.92
	KIAA0431	KIAA0431 protein	16q23.2	1.81
	CHST11	Carbohydrate (chondroitin 4) sulfotransferase 11	12q	1.78
	FLJ10613	Hypothetical protein FLJ10613	Xp11.22	1.76
	MGC29643	Hypothetical protein MGC29643	2q21.2	1.70
	FLJ21908	Hypothetical protein FLJ21908	12q13.11	1.64
	SMYD2	SET and MYND domain containing 2	1q32.3	1.57
	SIPL	SIPL protein	2p25.3	1.56
	LOC113251	c-Mpl binding protein	12q13.12	1.56
	JMJD1A	Jumonji domain containing 1A	2p11.2	1.53

Genes listed were within the Bonferroni adjusted confidence interval and have a fold change of 1.5-fold or greater. Genes were organized according to ontology as defined by Affymetrix's NetAffx online analysis center.

upon MEDII treatment (Table 2) and 20 genes were up-regulated in the MEDII-treated hESCs (Table 3). It is anticipated that fold change values reported when using a mixed linear model will tend to be lower than global fold change values that are reported in most array experiments [15]. This is attributed to a removal of all sources of systematic and random variation contributing to overall fluorescence intensity and the remaining differences in expression being due to the treatment variable alone.

To confirm differential gene expression with MEDII treatment, we analyzed seven genes by real-time PCR and their expression was as predicted by microarray analysis (Fig. 4). *POU5F1* and *NANOG* were not differentially expressed. *TDGF1* was up-regulated upon MEDII treatment with an average C_t difference of 1.5 (fold change of 3.0) over three independent passages. Both *HOXA1* and *DACT1* were down-regulated with an average C_t difference of 2.25 and 1.75 (fold change of 5.5 and 2.80), respectively, whereas *FST* and *EZH2* were down-regulated with an average C_t difference of 1.4 and 0.4 (fold change of 2.54 and 1.169), respectively.

Discussion

Knowledge gained from understanding the signaling events occurring in the embryo will likely lead to improved in vitro differentiation strategies for ES cells. This is the first report that describes early positive modulation of genes involved in vertebrate signaling pathway for mesoderm formation (*INHBE1*/*NODAL*/*TGFB1*) in hESCs. In this study, we have utilized an in vitro model of early ICM differentiation to hESCs exposed to MEDII medium. The treated cells expressed both pluripotent gene and candidate genes indicative of primitive streak cells and nascent mesoderm formation. By combining MEDII medium and microarray technologies we have taken a unique approach to: (1) characterize genes expressed by pluripotent hESCs in comparison to another pluripotent hESC from the

Table 3
Genes up-regulated after MEDII treatment of hESC

Functional category	Gene symbol	Gene description	Locus	Fold change
Cell adhesion	L1CAM	L1 cell adhesion molecule	Xq28	2.08
	ARHE	Ras homolog gene family, member E	2q23.3	2.07
	NK4	Natural killer cell transcript 4	16p13.3	1.78
	CDH3	Cadherin 3, type 1, P-cadherin (placental)	16q22.1	1.77
	TACSTD1	Tumor-associated calcium signal transducer 1	2p21	1.67
DNA binding	ZC3HDC1	Zinc finger CCCH type domain containing 1	7q34	1.81
Immune response	CD74	CD74 antigen	5q32	1.75
	HLA-DPA1	Major histocompatibility complex, class II, DP α 1	6p21.3	1.61
	HLA-B	Major histocompatibility complex, class I, B	6p21.3	1.50
Membrane-related	TM4SF2	Transmembrane 4 superfamily member 2	Xq11	1.79
Protein processing	PSMB8	Proteasome subunit, β type, 8	6p21.3	2.16
Signaling	TDGF1	Teratocarcinoma-derived growth factor 1	3p21.31	1.91
	GRPR	Gastrin-releasing peptide receptor	Xp22.2–p22.13	1.82
	AIP1	Atrophin-1 interacting protein 1	7q21	1.70
	NRP1	Neuropilin 1	10p12	1.52
Transcriptional regulation	EGR1	Early growth response 1	5q31.1	1.77
	DKFZp547K1113	Hypothetical protein DKFZp547K1113	15q26.1	1.61
Transport	MYO6	Myosin VI	6q13	1.69
Unknown	FLJ20171	Hypothetical protein FLJ20171	8q22.1	2.05
	FLJ20273	RNA-binding protein	4p13–p12	2.04

Genes listed were within the Bonferroni adjusted confidence interval and have a fold change of 1.5-fold or greater. Genes were organized according to ontology as defined by Affymetrix's NetAffx online analysis center.

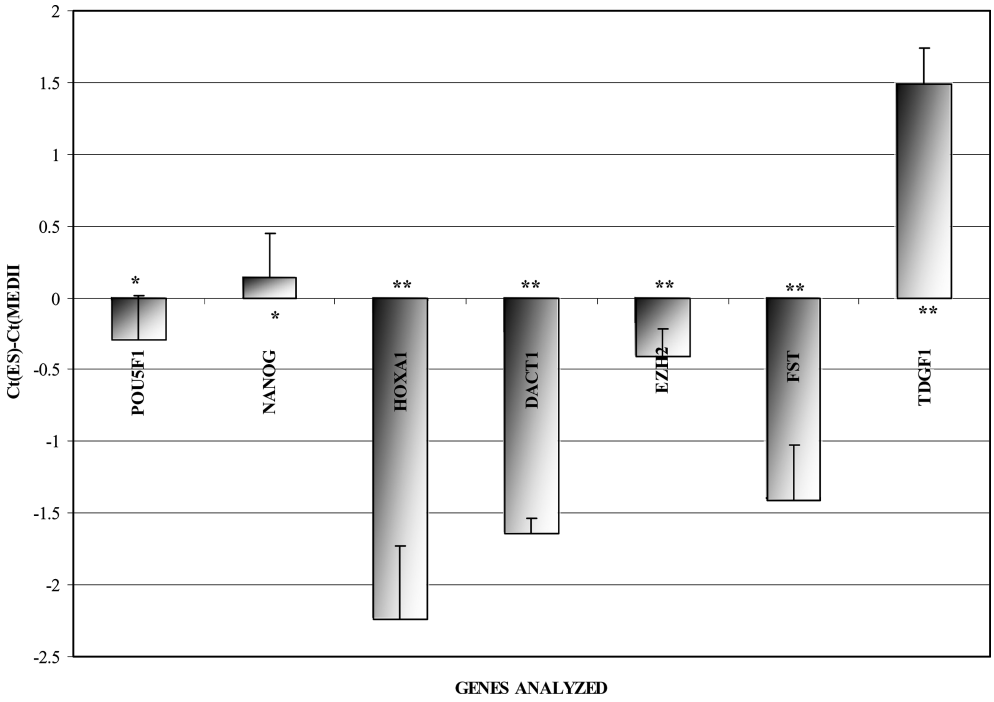

Fig. 4. Real-time PCR analysis of untreated and MEDII-treated hESCs. RNA used for real-time PCR was the same isolated for microarray analysis. C_t represents threshold cycle, the cycle at which fluorescence intensity is considered above background. The significance in differential gene expression and fold change was determined using REST software. *No observed fold change, while **a significant fold change. The *x*-axis is the genes analyzed and the *y*-axis is the average difference in C_t values between untreated and MEDII-treated hESC values from three replicates.

same parental population, and (2) investigate TGFB1/NODAL signaling pathway's gene expression in an in vitro model of embryo development. We have elucidated genes down-regulated in response to MEDII medium at a stage of differentiation before traditional pluripotency markers, such as *POU5F1*, *NANOG*, and SSEA-4, are down-regulated. In addition, MEDII-treated hESCs exhibited an up-regulation of several genes in the TGFB1/NODAL pathway, consistent with an activation of this pathway. Thus, further studies could produce a model to test the early and maybe the initial events in mesoderm induction in hESCs, prior to loss of *POU5F1* and *NANOG* expression.

Our initial results suggested that the response of hESCs to MEDII confirmed what was previously observed in the adherent mESC cultures. After 3 days in culture, MEDII-treated hESCs exhibited an obvious morphology difference in comparison to control hESCs at similar time-points. MEDII-treated hESC cell colonies were flatter and appeared less refractive than control hESCs. MEDII-treated hESCs also appeared to form tighter connections within colonies and no longer exhibited spaces between individual cells in a colony (Figs. 1A–D). MEDII-treated hESCs were also more resistant to dispersal to single cells during harvesting. This was also previously observed in MEDII-treated mES cell colonies that likewise formed a similar flattened colony phenotype [8]. Evaluation of the cell cycle profile of MEDII-treated and control hESCs revealed similarities with previously reported mESC cell cycle data. Mouse ES cells have a unique cell cycle profile with roughly 50% of cells analyzed residing in S phase and around 20% of cells occupying the G2/M phase of the cell cycle (19–21). Consistent with these findings, we found that hESCs have a higher proportion in the S and G2/M phases than in G1 when compared with the profiles of somatic mouse fibroblast cells (Fig. 2). It was further demonstrated that treatment with retinoic-acid (RA), a known neural differentiation inducing agent for mESCs, changes the cell cycle profile of mESCs to a profile more similar to terminally differentiated cells than epiblast cells [16]. However, MEDII-treated mESCs retain the unique cell cycle profile that is thought to be indicative of pluripotency [17]. Therefore, treatment of mESCs with terminal differentiation inducing agents drastically changes their cell cycle profile while MEDII treatment does not change the pluripotent cell cycle profile. Similarly, hESCs and MEDII-treated hESCs exhibit a cell cycle profile with many cells occupying the S and G2/M phases of the cell cycle, like the profile observed in untreated hESCs. Therefore, morphological alteration and cell cycle profiles of MEDII-treated hESC and mESCs are similar; suggesting that MEDII does not induce a program of terminal differentiation but instead may induce only early differentiation of hESCs at this point.

Previous studies with MEDII have shown that it causes differentiation to a second pluripotent population that is still POU5F1 positive, recapitulating events that occur in vivo in the mouse embryo [8]. After treatment of hESCs with MEDII medium, we observed an altered gene expression for many developmental, cell adhesion, and other genes. It is important to emphasize that alteration in gene expression occurred without changes in *POU5F1* and *NANOG* expression in cells that continued to retain their stem cell surface marker SSEA-4. Based on immunostaining results and morphological analysis, it appears that cells within the MEDII-treated hESC colonies were uniform; however, their altered gene expression profiles may not have been uniform, thus indicating that separate cell populations may have been responsible for the overall observed altered gene expression. Notwithstanding, MEDII did induce altered gene expression in several genes involved in primitive streak formation, and specific genes involved in the TGFB1/NODAL signaling pathway. Since MEDII-treated hESCs have unique features based on the differentially expressed genes, but unaltered in POU5F1 and NANOG gene expression and the cell surface marker SSEA-4, one can hypothesize that hESC populations are capable of being dynamic in nature without inherent changes in cell surface pluripotent markers. Therefore, the use of a handful of pluripotent markers may not be sufficient for characterizing a dynamic population of hESCs that is undergoing self-renewal and/or early differentiation.

The TGFB1/NODAL pathway is known to be important for primitive-streak and mesoderm formation, and the current study using MEDII is the only reported protocol for generating an in vitro cell population having both pluripotent gene expression and increased gene expression in this particular pathway. TDGF1 is a co-receptor/ligand of NODAL that was up-regulated upon MED II treatment. LEFTYA, an antagonist of NODAL/TDGF1 signaling normally expressed in the anterior visceral endoderm, is down-regulated with MEDII treatment [18]. Additionally, *FST* is down-regulated with MEDII treatment, with previous studies showing that FST may act as an inhibitor of mesoderm induction [19,20]. *GATA6* and *TBX1*, genes expressed in the primitive streak, are also up-regulated with MEDII treatment [21,22]. Taken together, these results indicate that MEDII affects a gene expression pattern consistent with anterior–posterior axis and primitive streak formation. In previous studies, MEDII treatment of mESCs that were then allowed to form cell aggregates or embryoid bodies had a higher degree of differentiation to mesoderm and further advanced mesoderm derived macrophages and cardiac muscle than non-treated mESCs, demonstrating the capability of MEDII to induce mesodermal differentiation [9]. It is important to note that this previous protocol used

embryoid bodies to look at a fully formed mesoderm, whereas we utilized an inherently more uniform monolayer approach to observe the initial events that may be directing the hESC toward differentiated states such as mesoderm.

In our studies, *TDGF1* was up-regulated in hESC colonies after 3 days exposure to MEDII, while down-regulated upon differentiation in other ES cell spontaneous differentiation studies [5]. Based on our microarray analysis, *TDGF1* was up-regulated 1.91-fold over the three independent passages in the study with a Bonferroni adjusted p value of 3.35×10^{-7}. Subsequently, increased expression was verified by real-time PCR with an average fold change of 3.01 over the three independent passages. *TDGF1* was initially identified as a gene in undifferentiated mouse and human teratocarcinoma cell lines whose expression decreased with retinoic acid treatment [23]. TDGF1 is a member of the EGF-CFC family of proteins that can act as either a co-receptor or co-ligand of the NODAL signaling pathway, by binding to a complex of ActRIB and ActRIIB receptors [24]. *TDGF1* has been shown to be initially expressed uniformly throughout the epiblast with further expression restricted to primitive streak epiblast cells and developing mesoderm [25,26]. Several functional studies have demonstrated the importance of *TDGF1* in early embryonic development. In studies utilizing *TDGF1* homozygous null mutant embryos, it was shown that TDGF1 was found to be essential for conversion of the proximal–distal axis to an anterior–posterior axis and streak formation. Mutant embryos failed to form a correct node, lacked a primitive streak, and did not form embryonic mesoderm properly [25,27]. Therefore, our results suggest that MEDII may be inducing very early differentiation signaling in the hESCs with *TDGF1* playing a role in this initial differentiation.

In association with TDGF1, DACT1, a Disheveled associated antagonist of CTNNB1 (β-catenin) was also downregulated in MEDII-treated hESCs. In a recently published report, characterization of gene expression in *CTNNB1* mutant embryos suggested a link with *TDGF1* expression [28]. The authors suggested that CTNNB1 up-regulates *TDGF1*, in turn increasing TDGF1 dependent NODAL signaling, through CTNNB1, during anterior–posterior axis formation. Ultimately, the increase in TDGF1 dependent NODAL signaling events activates mesoderm induction. Previous studies showed that increased levels of DACT1 resulted in decreased levels of soluble CTNNB1 and decreased activation of CTNNB1 responsive genes [29]. Therefore, our observed decrease in *DACT1* expression may enhance *CTNNB1* activity in MEDII-treated hESCs. Two genes observed as down-regulated by microarray analysis, *HOXA1* and *EZH2*, were also independently verified by real-time PCR analysis. HOX genes are a group of evolutionary conserved transcription factors arranged in clusters and expressed sequentially in both a spatial and temporal manner [30,31]. In human teratocarcinoma cells, *HOXA1* is the earliest HOX gene expressed after treatment with retinoic acid [32,33], with targeted disruption of the gene shown to be embryonic lethal [34]. *EZH2* (enhancer of zeste homolog 2), confirmed as differentially expressed in our analysis, is a polycomb-group gene that maintains chromatin status during differentiation thereby providing a transcriptional memory. Targeted disruption of the gene has been shown to be post-implantation lethal around the time of gastrulation. *EZH2* null blastocysts displayed impaired outgrowth, thereby inhibiting ES cell isolation [35]. Another gene of interest downregulated by MEDII treatment is Glypican-4 (*GPC4*) that has been reported as one of the 25 most significant genes in hESCs [6]. Examination of genes downregulated during the differentiation process before overt loss of pluripotency may thus provide a unique insight into genes operating in the pluripotent state.

In the current study, we have shown that MEDII affects early developmental gene expression in hESCs. Our results are in agreement with studies done in the mouse that have shown MEDII inducing a transitory state characterized by retention of pluripotent gene expression and change in the early embryo developmentally

A

GENE_ID	EXPRESSION	FUNCTION
Tbx-1 **	↑	Mesoderm formation
FST*	↓	Activin-binding inhibiting protein
GATA6**	↑	Primitive Streak/ Mesoderm formation
ZNFN1A1**	↑	Primitive Streak/ Mesoderm formation
EBAF*	↓	Nodal antagonist
TDGF-1*	↑	Nodal co-factor
DACT1*	↓	β-catenin antagonist

B

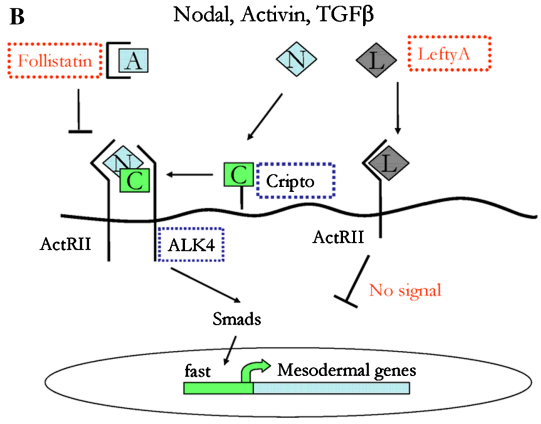

Fig. 5. (A) Expression of key genes in the primitive streak/nascent mesoderm upon treatment of hESCs with MEDII. Significant differences at a Bonferroni p value (*) and 0.001 (**) are indicated. (B) Proposed mesoderm induction model for MEDII effect on adherent hESCs. MEDII-treatment induced up-regulation of coligands and receptor gene expression (blue box) and down-regulation of inhibitory factor (red box) gene expression. A, activin; N, nodal; C, cripto; and L, leftyA. (For interpretation of the references to colour in this figure legend, the reader is referred to the web version of this paper.)

regulated genes [8]. Further, we have elucidated a set of genes down-regulated upon exposure to MEDII medium that may have a role in the pluripotent state of hESCs or the events leading to an exit in pluripotency. Consistent with this role, we have found changes in expression of several genes implicated in anterior–posterior axis formation, primitive streak formation, and early mesoderm induction (Fig. 5A). Based on our results it is possible that TDGF1 dependent TGFB1/NODAL signaling plays an early and important role in the initial differentiation from the pluripotent state towards the mesoderm fate (Fig. 5B). Treatment of hESCs with MEDII medium is the only reported differentiation protocol that shows an increase in *TDGF1* expression. This finding is important because failure to activate *TDGF1* during early differentiation leads to neural fate [36]; and since MEDII can exert this effect in monolayer culture, the resultant product will potentially be more uniform than the product of embryoid body differentiation protocols. Thus, continued differentiation with MEDII or isolation of the active mesoderm inducing factors might lead to more uniform mesoderm differentiation and play an important role in generating cell products destined for cellular replacement therapy.

Acknowledgments

The authors thank the Ovarian Cancer Institute for use of their Affymetrix microarray equipment. We also thank Mrs. Deb Weiler for feeder cell preparation and Mrs. Deanne Tibbetts for generation of MEDII medium. We also thank Ben Bolstad, Terry Speed, and Russ Wolfinger for valuable advice on analyzing Affymetrix array data. This work was supported in part by BresaGen Inc. and partial funding from the Georgia Tech/Emory Center (GTEC) for the Engineering of Living Tissues, an ERC Program of the National Science Foundation under Award No. EEC-9731643.

References

[1] R. Eiges, N. Benvenisty, A molecular view on pluripotent stem cells, FEBS Lett. 529 (2002) 135–141.
[2] M.J. Abeyta, A.T. Clark, R.T. Rodriguez, M.S. Bodnar, R.A. Pera, M.T. Firpo, Unique gene expression signatures of independently-derived human embryonic stem cell lines, Hum. Mol. Genet. 13 (2004) 601–608.
[3] B. Bhattacharya, T. Miura, R. Brandenberger, J. Mejido, Y. Luo, A.X. Yang, B.H. Joshi, I. Ginis, R.S. Thies, M. Amit, I. Lyons, B.G. Condie, J. Itskovitz-Eldor, M.S. Rao, R.K. Puri, Gene expression in human embryonic stem cell lines: unique molecular signature, Blood 103 (2004) 2956–2964.
[4] R.R. Rao, S.L. Stice, Gene expression profiling of embryonic stem cells leads to greater understanding of pluripotency and early developmental events, Biol. Reprod. (2004).
[5] N. Sato, I.M. Sanjuan, M. Heke, M. Uchida, F. Naef, A.H. Brivanlou, Molecular signature of human embryonic stem cells and its comparison with the mouse, Dev. Biol. 260 (2003) 404–413.
[6] J.M. Sperger, X. Chen, J.S. Draper, J.E. Antosiewicz, C.H. Chon, S.B. Jones, J.D. Brooks, P.W. Andrews, P.O. Brown, J.A. Thomson, Gene expression patterns in human embryonic stem cells and human pluripotent germ cell tumors, Proc. Natl. Acad. Sci. USA 100 (2003) 13350–13355.
[7] T.A. Pelton, S. Sharma, T.C. Schulz, J. Rathjen, P.D. Rathjen, Transient pluripotent cell populations during primitive ectoderm formation: correlation of in vivo and in vitro pluripotent cell development, J. Cell Sci. 115 (2002) 329–339.
[8] J. Rathjen, J.A. Lake, M.D. Bettess, J.M. Washington, G. Chapman, P.D. Rathjen, Formation of a primitive ectoderm like cell population, EPL cells, from ES cells in response to biologically derived factors, J. Cell Sci. 112 (Pt. 5) (1999) 601–612.
[9] J. Lake, J. Rathjen, J. Remiszewski, P.D. Rathjen, Reversible programming of pluripotent cell differentiation, J. Cell Sci. 113 (Pt. 3) (2000) 555–566.
[10] J. Rathjen, B.P. Haines, K.M. Hudson, A. Nesci, S. Dunn, P.D. Rathjen, Directed differentiation of pluripotent cells to neural lineages: homogeneous formation and differentiation of a neurectoderm population, Development 129 (2002) 2649–2661.
[11] J.D. Calhoun, N.A. Lambert, M.M. Mitalipova, S.A. Noggle, I. Lyons, B.G. Condie, S.L. Stice, Differentiation of rhesus embryonic stem cells to neural progenitors and neurons, Biochem. Biophys. Res. Commun. 306 (2003) 191–197.
[12] T.C. Schulz, G.M. Palmarini, S.A. Noggle, D.A. Weiler, M.M. Mitalipova, B.G. Condie, Directed neuronal differentiation of human embryonic stem cells, BMC Neurosci. 4 (2003) 27.
[13] M. Mitalipova, J. Calhoun, S. Shin, D. Wininger, T. Schulz, S. Noggle, A. Venable, I. Lyons, A. Robins, S. Stice, Human embryonic stem cell lines derived from discarded embryos, Stem Cells 21 (2003) 521–526.
[14] R.A. Irizarry, B.M. Bolstad, F. Collin, L.M. Cope, B. Hobbs, T.P. Speed, Summaries of affymetrix genechip probe level data, Nucleic Acids Res. 31 (2003) e15.
[15] T.M. Chu, B. Weir, R. Wolfinger, A systematic statistical linear modeling approach to oligonucleotide array experiments, Math Biosci. 176 (2002) 35–51.
[16] L. Jirmanova, M. Afanassieff, S. Gobert-Gosse, S. Markossian, P. Savatier, Differential contributions of ERK and PI3-kinase to the regulation of cyclin D1 expression and to the control of the G1/S transition in mouse embryonic stem cells, Oncogene 21 (2002) 5515–5528.
[17] E. Stead, J. White, R. Faast, S. Conn, S. Goldstone, J. Rathjen, U. Dhingra, P. Rathjen, D. Walker, S. Dalton, Pluripotent cell division cycles are driven by ectopic Cdk2, cyclin A/E and E2F activities, Oncogene 21 (2002) 8320–8333.
[18] A.F. Schier, Nodal signaling in vertebrate development, Annu. Rev. Cell Dev. Biol. 19 (2003) 589–621.
[19] M. Levin, The roles of activin and follistatin signaling in chick gastrulation, Int. J. Dev. Biol. 42 (1998) 553–559.
[20] L. Marchant, C. Linker, R. Mayor, Inhibition of mesoderm formation by follistatin, Dev. Genes Evol. 208 (1998) 157–160.
[21] D.L. Chapman, N. Garvey, S. Hancock, M. Alexiou, S.I. Agulnik, J.J. Gibson-Brown, J. Cebra-Thomas, R.J. Bollag, L.M. Silver, V.E. Papaioannou, Expression of the T-box family genes, Tbx1–Tbx5, during early mouse development, Dev. Dyn. 206 (1996) 379–390.
[22] E.E. Morrisey, H.S. Ip, M.M. Lu, M.S. Parmacek, GATA-6: a zinc finger transcription factor that is expressed in multiple cell lineages derived from lateral mesoderm, Dev. Biol. 177 (1996) 309–322.
[23] A. Ciccodicola, R. Dono, S. Obici, A. Simeone, M. Zollo, M.G. Persico, Molecular characterization of a gene of the 'EGF family' expressed in undifferentiated human NTERA2 teratocarcinoma cells, EMBO J. 8 (1989) 1987–1991.

[24] C. Bianco, C. Wechselberger, A. Ebert, N.I. Khan, Y. Sun, D.S. Salomon, Identification of Cripto-1 in human milk, Breast Cancer Res. Treat. 66 (2001) 1–7.
[25] J. Ding, L. Yang, Y.T. Yan, A. Chen, N. Desai, A. Wynshaw-Boris, M.M. Shen, Cripto is required for correct orientation of the anterior–posterior axis in the mouse embryo, Nature 395 (1998) 702–707.
[26] R. Dono, L. Scalera, F. Pacifico, D. Acampora, M.G. Persico, A. Simeone, The murine cripto gene: expression during mesoderm induction and early heart morphogenesis, Development 118 (1993) 1157–1168.
[27] C. Xu, G. Liguori, M.G. Persico, E.D. Adamson, Abrogation of the Cripto gene in mouse leads to failure of postgastrulation morphogenesis and lack of differentiation of cardiomyocytes, Development 126 (1999) 483–494.
[28] M. Morkel, J. Huelsken, M. Wakamiya, J. Ding, M. van de Wetering, H. Clevers, M.M. Taketo, R.R. Behringer, M.M. Shen, W. Birchmeier, Beta-catenin regulates Cripto- and Wnt3-dependent gene expression programs in mouse axis and mesoderm formation, Development 130 (2003) 6283–6294.
[29] B.N. Cheyette, J.S. Waxman, J.R. Miller, K. Takemaru, L.C. Sheldahl, N. Khlebtsova, E.P. Fox, T. Earnest, R.T. Moon, Dapper, a Dishevelled-associated antagonist of beta-catenin and JNK signaling, is required for notochord formation, Dev. Cell 2 (2002) 449–461.
[30] B. Favier, P. Dolle, Developmental functions of mammalian Hox genes, Mol. Hum. Reprod. 3 (1997) 115–131.
[31] M. Maconochie, S. Nonchev, A. Morrison, R. Krumlauf, Paralogous Hox genes: function and regulation, Annu. Rev. Genet. 30 (1996) 529–556.
[32] R. Buettner, S.O. Yim, Y.S. Hong, E. Boncinelli, M.A. Tainsky, Alteration of homeobox gene expression by N-ras transformation of PA-1 human teratocarcinoma cells, Mol. Cell. Biol. 11 (1991) 3573–3583.
[33] A. Simeone, D. Acampora, L. Arcioni, P.W. Andrews, E. Boncinelli, F. Mavilio, Sequential activation of HOX2 homeobox genes by retinoic acid in human embryonal carcinoma cells, Nature 346 (1990) 763–766.
[34] T. Lufkin, A. Dierich, M. LeMeur, M. Mark, P. Chambon, Disruption of the Hox-1.6 homeobox gene results in defects in a region corresponding to its rostral domain of expression, Cell 66 (1991) 1105–1119.
[35] D. O'Carroll, S. Erhardt, M. Pagani, S.C. Barton, M.A. Surani, T. Jenuwein, The polycomb-group gene Ezh2 is required for early mouse development, Mol. Cell. Biol. 21 (2001) 4330–4336.
[36] S. Parisi, D. D'Andrea, C.T. Lago, E.D. Adamson, M.G. Persico, G. Minchiotti, Nodal-dependent Cripto signaling promotes cardiomyogenesis and redirects the neural fate of embryonic stem cells, J. Cell Biol. 163 (2003) 303–314.